During natural viewing, neural processing of visual targets continues throughout saccades

Atanas D. Stankov Department of Biomedical Engineering, City College of New York, New York, NY, USA

Jonathan Touryan U.S. Army Research Laboratory, Aberdeen Proving Ground, MD, USA

Stephen Gordon DCS Corp., Alexandria, VA, USA

Anthony J. Ries U.S. Army Research Laboratory, Aberdeen Proving Ground, MD, USA

Jason Ki Department of Biomedical Engineering, City College of New York, New York, NY, USA

Lucas C. Parra Department of Biomedical Engineering, City College of New York, New York, NY, USA

Relatively little is known about visual processing during free-viewing visual search in realistic dynamic environments. Free-viewing is characterized by frequent saccades. During saccades, visual processing is thought to be suppressed, yet we know that the presaccadic visual content can modulate postsaccadic processing. To better understand these processes in a realistic setting, we study here saccades and neural responses elicited by the appearance of visual targets in a realistic virtual environment. While subjects were being driven through a 3D virtual town, they were asked to discriminate between targets that appear on the road. Using a system identification approach, we separated overlapping and correlated activity evoked by visual targets, saccades, and button presses. We found that the presence of a target enhances early occipital as well as late frontocentral saccade-related responses. The earlier potential, shortly after 125 ms post-saccade onset, was enhanced for targets that appeared in the peripheral vision as compared to the central vision, suggesting that fast peripheral processing initiated before saccade onset. The later potential, at 195 ms post-saccade onset, was strongly modulated by the visibility of the target. Together these results suggest that, during natural viewing, neural processing of the presaccadic visual stimulus continues throughout the saccade, apparently unencumbered by saccadic suppression.

Introduction

Visual perception in the natural world requires the processing of a dynamic stimulus, with moving objects and an ever-changing perspective as the result of head and eye movements. To recreate some of this visual dynamic, recent work on visual perception uses movies and video games allowing subjects to freely scan the scene while recording brain activity and eye movements (Barczak, Haegens, Ross, McGinnis, Lakatos, & Schroeder, 2019; Dorr, Martinetz, Gegenfurtner, & Barth, 2010; Gordon, Jaswa, Solon, & Lawhern, 2017; Konstantopoulos, Chapman, & Crundall, 2010). Free-viewing is dominated by frequent saccades, which are fast eye movements that serve to update the visual input (Barczak et al., 2019; Dorr et al., 2010).

Both the saccade as well as the new visual input from the subsequent fixation produce a large post-saccadic enhancement in brain activity, which can be measured

Citation: Stankov, A. D., Touryan, J., Gordon, S., Ries, A. J., Ki, J., & Parra, L. C. (2021). During natural viewing, neural processing of visual targets continues throughout saccades. *Journal of Vision*, *21*(10):7, 1–14, https://doi.org/10.1167/jov.21.10.7.

https://doi.org/10.1167/jov.21.10.7 Received January 25, 2021; published September 7, 2021 ISSN 1534-7362

as evoked potentials on the scalp (Buonocore, Dimigen & Melcher, 2020; Ehinger, König, & Ossandón, 2015; Guérin-Dugué, Roy, Kristensen, Rivet, Vercueil, & Tcherkassof, 2018; Kazai & Yagi, 2003). Postsaccadic potentials are also known to be affected by features of the stimulus before a saccade, either in the saccade-locked event-related potentials (ERPs) or the fixation related potential (FRPs). Some of these studies use classic experimental paradigms with artificial stimuli that intentionally constrain fixations and saccades (Brouwer, Reuderink, Vincent, van Gerven, & van Erp, 2013; Buonocore et al., 2020; Ehinger et al., 2015; Hiebel, Ischebeck, Brunner, Nikolaev, Höfler, & Körner, 2018; Kazai & Yagi, 2003; Peterburs, Gajda, Hoffmann, Daum, & Bellebaum, 2011; Purcell, Heitz, Cohen, & Schall, 2012) while others use more realistic tasks, such as reading (Dimigen, Kliegl, & Sommer, 2012) or natural images without restricting saccades (Devillez, Guyader, & Guérin-Dugué, 2015; Guérin-Dugué et al., 2018; Rämä & Baccino, 2010). Interestingly, there is also substantial evidence that, during saccades, visual processing is suppressed and subjects fail to detect changes in the visual scene or experience compressed perception (Castet & Masson, 2000; Ibbotson & Krekelberg, 2011; Ross, Morrone, & Burr, 1997; Ross, Morrone, Goldberg, & Burr, 2001). Conversely, after a saccade, detection performance, as well as neural activity, are enhanced as a function of presaccadic stimuli (Dorr & Bex, 2013; MacEvoy, Hanks, & Paradiso, 2008). There is also behavioral evidence for a shift of attention toward a target location starting before saccade onset (Deubel, 2008; Jonikaitis, Szinte, Rolfs, & Cavanagh, 2012). Therefore, processing of the visual stimulus appears to start prior to the saccade, is suppressed during, and continues with enhancement after the saccade (Ibbotson, Crowder, Cloherty, Price, & Mustari, 2008). This literature spans classic experimental paradigms and free viewing of static natural images, but few of these studies deal with naturalistic tasks and natural dynamic stimuli, such as video. Thus, the effect of the presaccadic stimulus on the post-saccading processing in dynamic natural stimuli is less well understood.

We hypothesize that during a natural vision in dynamic environments there is a continuity of visual processing across a saccade. We, therefore, predicted that the visual stimulus prior to a saccade modulates the post-saccading processing, as has been observed for static images. To test this, we use a target discrimination task embedded in a dynamic virtual environment, while we record eye movements and electroencephalogram (EEG). Here, objects were presented on the road while subjects are being driven through a 3D virtual town (Gordon et al., 2017). They are asked to distinguish between threatening and nonthreatening targets that suddenly appear in the environment. To test our predictions, we analyzed saccade-evoked potentials to determine if they are affected by the presentation of targets, their visibility, and their location in the visual field. We used a systems identification approach to disentangle the overlapping responses to target presentation, saccades, and motor response typical for a naturalistic task under free viewing conditions. Our results suggest that neural processing of the visual stimulus, including reorienting, starts before a saccade and continues throughout the saccade without introducing delays. To our knowledge, it is the first study to demonstrate this continuity of neural processing with natural dynamic stimuli and in human subjects.

Methods

Data collection and procedure

Healthy, right-handed male subjects between the ages of 20 and 40 (mean = 28.3) were recruited among Army Research Laboratory (ARL) and other government employees. Subjects gave informed consent in accordance with the requirements of the Institutional Review Board of the ARL in accordance with 32 Code of Federal Regulation (CFR) 219 and AR 70-25, and also in compliance with the Declaration of Helsinki. The experiment was conducted in an electrically shielded, sound-dampened room. Prior to the primary experimental task, subjects performed an eye-calibration (see below). For the primary experimental task, subjects were driven around a simulated 3D environment and were required to discriminate human entities as either a nontarget (an image of a man) or a target (an image of a man with a gun) and tables as either a nontarget (an image of a table with a clear view under it) or a target (an image of a table with an obstructed view of the space under it). Stimuli were presented for 1 second with an inter-stimulus interval (ISI) of 2 ± 0.5 seconds. For each target the subject responded by pushing a button with the left or right hand to indicate the target type. The button used to indicate target type (left or right) was counterbalanced across subjects in an alternating fashion. Participants were instructed to use the right index finger for pressing the right button and the left index finger for the left button.

Experimental stimuli and task description

The subject was presented with 300 human and 300 table targets. These 600 targets were split into two successive runs. In other words, during the first 15-minute block of the experiment, the subjects encountered targets 1 to 300. During the second 15-minute block the subjects encountered targets 301

to 600. The location and placement of targets were randomly predefined and were held consistent across all subjects. In other words, each subject saw the same target at the same location. The order of presentation of 15-minute blocks was counterbalanced across subjects. The location in which targets appeared was visually verified during pilot testing to be at logical locations (i.e. level with the ground plane and with an unobstructed line of sight).

During each block visibility conditions were altered through the use of a fog-like overlay on the image. Throughout each block the fog would appear for a few seconds, up to a minute, and then disappear.

Finally, during each 15-minute block, the subject's scores were presented on the bottom of the screen. Subjects were instructed to try to beat a virtual competitor. Unbeknownst to the subject, the virtual competitor's score was adjusted to follow the subject's score with extended time frames when the participant was winning or losing. In the easy condition, this difference was such that the player was winning most of the time, including at the end. During the hard condition, the virtual competitor was winning about half the time and would often win at the end.

Equipment

The EEG configuration was a 64-Channel Biosemi Active II (Amsterdam, The Netherlands) recorded at 1024 Hz. Online referencing was done to the Common Mode Sense electrode, which was later offline re-referenced to the mastoid electrodes. Eye tracking was done using a 60 Hz eye-tracker faceLAB 4.2 by Seeing Machines (Fystick, Australia). External electrodes from the BioSemi system were placed on both mastoids for signal reference, next to the outer canthus of each eye to record horizontal electrooculogram (EOG), and directly below the left eye in the inferior orbital margin to obtain a differential vertical EOG record when paired with the signal from the Fp1 electrode in the standard 64 channel montage. Additional external electrodes were placed at the top and bottom of the left masseter jaw muscle, and below the left breast to obtain a basic electrocardiogram (ECG) waveform.

EEG preprocessing

EEG was filtered with a 0.3 to 250 Hz bandpass filter and eye-movement artifacts were corrected by regressing out a single left vertical and a single right horizontal EOG channels and two left frontal channels (Fp1 and AF7; for display purposes Fp1 and AF7 were replaced with their right side mirror opposites Fp2 and AF8). Subsequently, we used robust principal component analysis (Candès, Li, Ma, & Wright, 2011), which implicitly removes outlier channels and myographic activity. EEG was downsampled to 256 Hz for temporal response function analysis. All data preprocessing and analysis were implemented in MATLAB.

Gaze position

Eye tracking data was used to determine target location relative to gaze position. For this purpose, raw eye tracking data (60 Hz sampling frequency) were calibrated to the 1024 by 768 pixel space of the screen by using the calibration tasks prior to the main experiment. Then they were asked to look at dots that appear in random sequence at the four corners or the center of the screen and click with the mouse when the dot appears. The gaze coordinates at the time of the mouse clicks were used to create an affine transform that maps the gaze position to screen coordinates of the corresponding dots. To reduce variance in the gaze position, we applied a temporal filter (rectangular window of size 0.25 seconds). The result was validated using gaze position data collected during a smooth-pursuit task (follow a slowly moving ball on the screen). The screen size was 24 inches (51.1 $\times$ 29.9 cm) and subjects were seated approximately 60 cm from the screen resulting in a visual stimulus that covers approximately 44.2 degrees by 33.9 degrees in visual angle.

Saccade detection

Saccade's onset times and duration were detected from the EOG because recordings of the eye position did not have sufficient temporal resolution after temporal smoothing. Specifically, we used a saccade detection algorithm based on EOG activity (Toivanen, Pettersson, & Lukander, 2015) and applied it here to the raw EOG signal (horizontal minus vertical channels) at a resolution of 1024 Hz.

Statistical tests

For matched data comparisons (saccade/button response times, number of saccades, and target discrimination accuracy), we used a signed-rank test and for unmatched data comparisons (saccade amplitude) we used a rank-sum test. In addition, to test the uniformity saccades and button response histograms of the task trial we used a chi-squared test.

Data analysis

Temporal response functions (TRFs) were used to derive overlapping evoked responses using a conventional linear system identification approach. This approach assumes that all the responses during the target trials are a linear superposition of five types of events. The presentation of the target, button responses, and saccades, which were further divided into those following the target (100 and 450 ms), those within 1 second of the target presentation but outside this range, and spontaneous saccades, which are more than 1 second away from the target. Each type of response has a stereotypic temporal response filter (TRF, equivalent to an impulse response) that when convolved with all the onsets of each respective event and added together across event types will produce an estimate of EEG signal. Algebraically the convolution is constructed by the following matrix multiplication:

$$y = Xb,$$

where X is a binary Toeplitz matrix indicating when events happen, b are the TRFs, and y is the estimated EEG time series. The Toeplitz matrix implements the convolution and can be concatenated to form a block-Toepliz matrix that implements the sum over the five event types:

$$X = [X_1 X_2 X_3 X_4 X_5] \text{ and } b = [b_1 b_2 b_3 b_4 b_5].$$

To derive the TRFs we use conventional least-squares optimization:

$$\hat{b} = (X^T X)^{-1} X^T Y = {R_{xx}}^{-1} R_{xy}.$$

R_{xx} and R_{xy} are the auto- and cross-correlation matrices of x and y. R_{xy} captures the conventional trial-averaged evoked responses. The inverse of R_{xx} removes correlation induced but correlated events and responses that overlap in time. For memory efficiency, the construction and multiplication of X are done using sparse matrix form in MATLAB before switching back to full matrix form for R_{xx} and R_{xy}. For further memory efficiency, the TRFs were computed for each subject individually and then averaged across subjects to give the group estimate TRF. Before averaging across subjects, each TRF was baseline corrected using the 125 ms before onset.

The approach used here is essentially a classic multiple-input single-output (MISO) system's identification approach. To our knowledge it has been the first used for EEG in the context of continuous stimuli driving evoked responses (Crosse, Di Liberto, Bednar, & Lalor, 2016; Lalor, Pearlmutter, Reilly, McDarby, & Foxe, 2006). In contrast to this previous work, we found no need to regularize the inverse of R_{xx}, which is sometimes done to reduce noise. The same approach has also been used to disentangle overlapping responses of consecutive eye movements (Dandekar, Privitera, Carney, & Klein, 2011; Dimigen & Ehinger, 2021; Guérin-Dugué et al., 2018). The work of Dimigen and Ehinger extend the approach by including classic interaction terms to determine if different types of events influence each other (multiplicatively). In that work, a TRF is estimated for each type of event and a separate TRF is estimated to capture the difference between conditions. In contrast, here, we estimate a TRF for each condition separately and then take a difference. Given the linearity of the model, these approaches are equivalent (except for the interaction terms, which we do not use here).

For the analysis of spontaneous versus target-evoked saccades, we estimated a single model b using the data from the clear condition and fog condition. For the comparison of fog and clear conditions a separate model, b, was estimated for each condition. For the comparison of central and peripheral targets, we estimate a separate model, b, for each type of saccade.

Statistical significance of contrast in the TRFs between different conditions were determined using a permutation test. The 500 surrogate contrasts were created by shuffling trials between conditions. This was done for the contrasts in saccade type, target visibility, target location, and target threat type. To compare across game difficulty, 500 surrogates were created by shuffling subjects between the two game difficulties (not shown). Across 64 channels and 320 time points (spanning −250 to 1000 of the trial) there were 20,480 individual tests that were false discovery rate (FDR) corrected (Benjamini & Hochberg, 1995) with an alpha of 0.05.

Results

Subjects ($N = 16$) perform a target-detection task that involves discrimination of objects as a vehicle navigates through an urban environment (Figure 1A). Participants were asked to discriminate between threatening and nonthreatening targets (Figure 1E), which appear along the road at random intervals of 1 second to 3 seconds (Figure 1B). They respond with a button press using either the left or right hand (counterbalanced across subjects). The game is presented in four different conditions: fog versus clear visibility (see Figures 1A, 1C) as well as "easy" versus "hard". Subjects receive feedback on their discrimination performance in real-time as a numerical score on the screen, along with

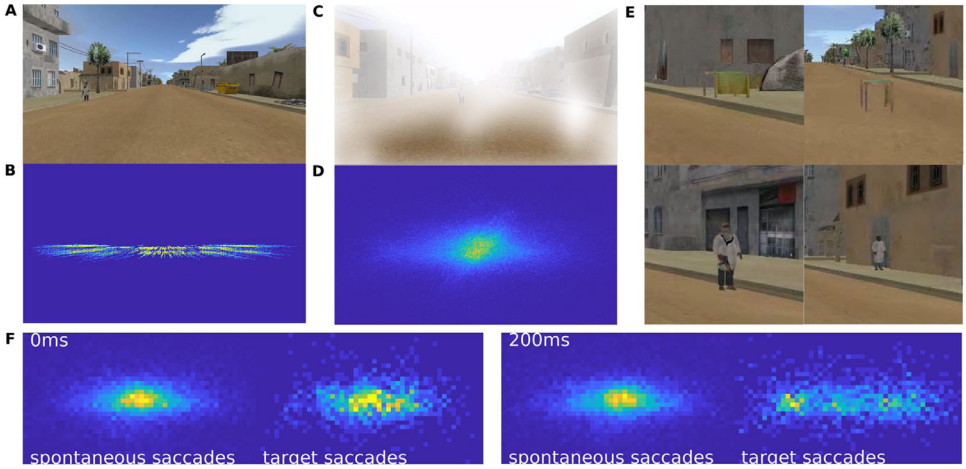

Figure 1. **Visual environment and target discrimination task.** (**A**) In the discrimination task, subjects detect "targets" appear along the road in an urban environment. (**B**) Distribution of target positions for 15 minutes of play. Targets move outwards as a result of forward movement of the viewer. (**C**) Subjects play the game in a clear visibility condition, as well as a fog condition. (**D**) Distribution of gaze position averaged over 14 subjects for 15 minutes of play. (**E**) Subjects are asked to report with a button push if the target is a "threat" (left panel: covered table and armed man) or if the target is a "non-threat" (right panel: clear table or unarmed man). (**F**) Eye gaze positions at 0 and 200 ms post-saccade onset for spontaneous and target-evoked saccades. Target gaze goes from the center of the screen at 0 ms to the left and right by 200 ms as the subjects shift their eyes to the target locations. The target-related eye gaze distribution at 200 ms overlaps with the target presentation distribution as shown in panel **B**.

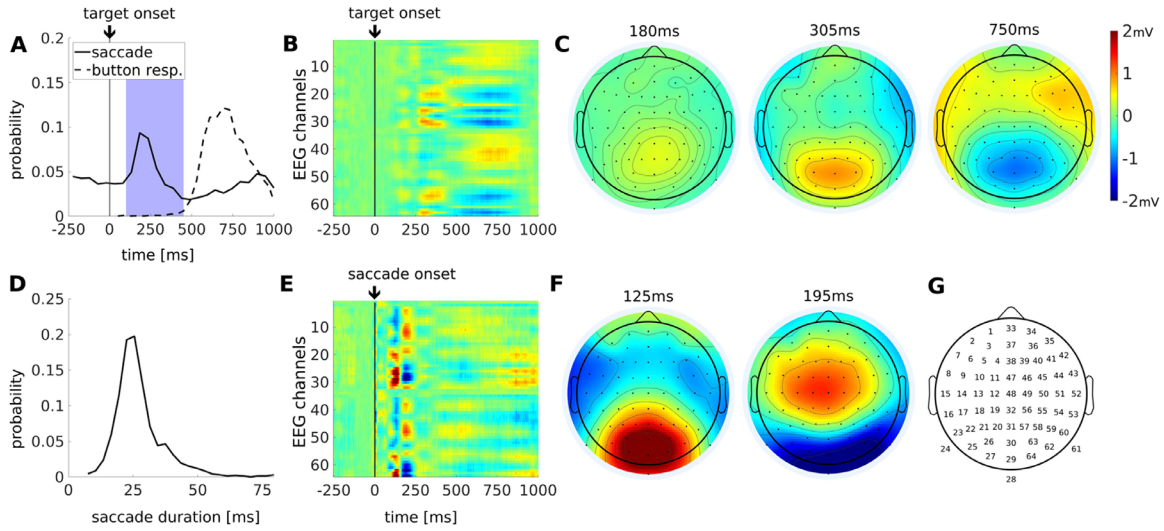

Figure 2. **Behavioral and neural responses across all subjects and conditions for trials with a button response.** (**A**) Button response times (dotted line) and all detected saccades (solid line) within the same trials, which can include multiple saccades per trial. Target-evoked saccades (blue shaded time interval, 100–450 ms) are selected for comparison with spontaneous saccades. (**B**) Temporal response function (TRF) locked to target presentations ($N = 4035$). Black line at 0 ms demarcates target onset. (**C**) Spatial distribution of target-locked TRF at 180 ms, 305 ms, and 750 ms. (**D**) Histograms for the duration of all target evoked saccades. (**E**) Saccade-related TRF for saccades following the presentation of a target (100–450 ms, $N = 1749$). Black line at 0 ms demarcates saccade onset. (**F**) Topographic snapshots at 125 and 195 ms. Color map indicates mV identically in all panels **B**, **C**, **E**, and **F**. (**G**) Headcap with electrode numbers used in the study.

the scores of a virtual competitor. In the "easy" condition, the virtual competitor is matched in performance, whereas in the "hard" condition the competitor usually outperforms the player. Each condition presents 300 targets (or "trials") and lasts 15 minutes. During play game, we recorded 64 channels of EEG (Figure 2G), eye movements, and button responses.

Target presentation elicits saccades

To assess the eye movement and behavioral response during the discrimination task, we analyze gaze position, saccades, and button response times. Gaze position was focused at the center of the screen (Figure 1D) and subjects reoriented their gaze with a saccade, which is reflected by an increase in saccade probability between 100 and 450 ms following target onset (Figure 2A, blue shading). We will refer to saccades in this temporal window as "target-evoked saccades." Target-evoked saccades tend to move the gaze toward the targets, whereas spontaneous saccades do not have a preferred direction (Figure 1F). This is followed by a drop in saccade probability, that is likely the result of a post-saccadic refractory period (Otero-Millan, Troncoso, Macknik, Serrano-Pedraza, & Martinez-Conde, 2008). The button responses following target presentation mainly occurred after 500 ms (see Figure 2A, dotted histograms). The timing of target-evoked saccades does not correlate with button response times (Supplementary Figure S1; Spearman correlation: $r = 0.012$, $p = 0.59$, $N = 1749$), suggesting that response times are not affected by the saccade. However, saccades and button responses are tightly coupled to the target presentation (see Figure 2A; i.e. the saccade and bottom response histograms are non-uniform [X-square test for saccades times: $X^2(24, N = 25) = 1016.5$, $p < 0.00$; for button response times $X^2(24, N = 25] = 4840.7$, $p < 0.00$).

Estimating target-evoked saccades, target-evoked potentials, and saccade-evoked potentials

Neural responses elicited during the discrimination task are characterized by multiple events (e.g. target presentation, saccades, and button responses). These events are correlated with one another (see Figure 2A) and the associated neural responses overlap in time. Therefore, simple trial averaging conventionally used to compute event related potentials cannot extract the unique contributions of each of these events. Thus, we use a system identification approach to identify the individual contributions of each event to the evoked potentials (see the Methods section). In this approach, each event contributes additively a "temporal response function" (or impulse response) to the evoked potentials. The TRFs are estimated simultaneously while taking into account correlation between different events and time points. A similar approach has been used to deconvolve overlapping responses to continuous naturalistic visual experience that involve dynamic visual input neural signals (Crosse et al., 2016; Lalor et al., 2006) and eye movements (Dandekar et al., 2011; Dimigen & Ehinger, 2021; Guérin-Dugué et al., 2018).

Target-evoked saccades elicit unique neural response

First, we assess the effect of target-evoked saccade on evoked neural response. Here, we compute the overall TRF for each event by combining trials from all subjects and conditions. In this and all subsequent analyses, we only consider trials that were followed by a button response. The TRF evoked by the target onset (Figure 2B) reveals an initial positive potential which starts occipitally moving anteriorly to parietal electrodes in the period of 250 ms to 450 ms (Figure 2C). This is followed by occipital negativity and centro-frontal positivity around the time of the button push at 550 ms to 850 ms (see Figure 2C). The initial occipital responses expected following a visual stimulus – C1 and P1 starting at 75 ms (Clark, Fan, Hillyard, 1994) – are not evident here. Instead, the first target-evoked response peaks at 180 ms and is more central and anterior than the conventional P1; (compare Figure 2C to e.g. Novitskiy, Ramautar, Vanderperren, De Vos, Mennes, Mijovic, Vanrumste, Stiers, Van den Bergh, Lagae, Sunaert, Van Huffel, & Wagemans, 2011). Perhaps this is due to the overlapping saccades, elicited by the target onset, starting at 100 ms.

The TRF for these target-evoked saccades (Figure 2E, and as time courses in Supplementary Figure S3) resembles the temporal dynamic of the "lambda complex" (Marton, Szirtes, & Breuer, 1985; Yagi, 1979). However, the precise timing and spatial distribution differ from the conventional lambda complex. Here, the occipital positivity peaks earlier, at 125 ms, perhaps due to differences in saccade duration (Yagi, 1979). In the present study, the mean saccade duration is approximately 27 ms with a range of durations around this mean (Figure 2D). For these target-evoked saccades, a second TRF peak appears at 195 ms, which is not evident for generic saccades (e.g. during a free-viewing image search task; Dias, Sajda, Dmochowski, & Parra, 2013). With the majority of saccades starting 200 ms after target presentation, this puts the peak at 400 ms.

Saccades following a target elicit stronger saccade-related TRF amplitudes

To highlight the difference in neural activity between spontaneous saccades and those evoked by the target, we compared saccade-related TRFs in the presence or absence of a target. Specifically, we subtracted the TRF for target-evoked saccades (see Figure 3A) from the TRF of spontaneous saccades (see Figure 3B). There are significant differences up to 650 ms following the saccade (Figure 3C), which our system-identification approach did not attribute to the button response (see Supplementary Figure S2) that follows nearly all target-evoked saccades. Focusing on the time period

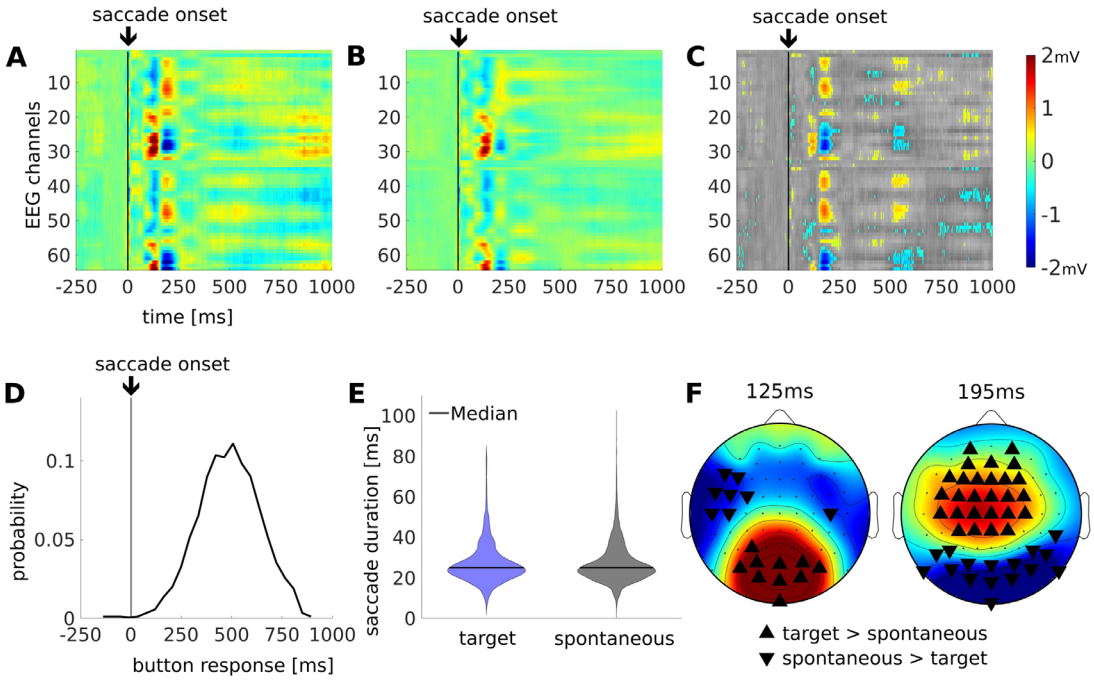

Figure 3. **Differences in saccade-related TRFs between spontaneous and target elicited saccades.** (**A**) TRF for target-evoked saccades ($N = 1749$), which are defined as saccades within 100 to 450 ms after target presentation. (**B**) TRF for spontaneous saccades ($N = 12{,}437$), which are those saccades not preceded by a target for at least 1000 ms. (**C**) The difference in saccade-related TRF between target-evoked minus spontaneous saccades. Significant differences are shown in color, superimposed on nonsignificant differences in gray. Significance is computed by permuting event onsets between the two conditions 500 times. This provides a surrogate distribution at which a two-tailed significance was determined at $p < 0.05$ after false-discovery rate correction for multiple comparisons. Color map indicates mV identically in all panels **A** to **D**, however, in panel **C**, color indicates voltage difference between types of saccades. (**D**) Button response times distribution with respect to saccade onset. (**E**) Density plots of saccade durations for target-evoked and spontaneous saccades. (**F**) Spatial distribution of the TRF difference at 125 ms and 195 ms.

before the button push (see Figure 3D), we find significant enhancement of the same two peaks at 125 ms and 195 ms (see Figure 3F). Early saccade-evoked potentials are known to be modulated with saccade amplitude (Yagi, 1979). Note that saccade duration did not differ between target-evoked and spontaneous saccades (see Figure 3E; rank-sum test: $z = -0.36$, $p = 0.71$), which rules out saccade amplitude as a confounding factor (amplitude and duration correlate). Instead, it is the presence of the target that enhances saccade-related TRFs as early as 125 ms after saccade onset.

Target visibility affected late but not early saccade-related TRFs

We expected that poor visibility (low contrast targets) would result in slower button responses and weaker evoked responses as compared to the clear visibility condition (high contrast targets). In the fog condition, subjects were significantly slower in their target-evoked saccades (see Figure 4D; signed-rank test: $z(15) = 2.79$, $p = 0.0052$) and button responses (see Figure 4E; signed-rank test: $z(15) = 3.15$, $p = 0.0016$) as compared to the clear condition. To test for differences in evoked responses, we subtracted the target-related TRFs of the clear visibility conditions (see Figure 4A) from that of the fog condition (see Figure 4B). We see significant differences starting at 150 ms and lasting at least until 1 second after target onset (see Figure 4C). As expected, differences reflect a drop in TRFs magnitude for the fog conditions (i.e. positivity increases and negativity decreases; see Figure 4F).

Saccade-locked responses to the clear and foggy conditions both show robust response (see Figures 4G, 4H respectively). In computing the differences for the saccade-locked potentials (see Figure 4I), we see both early and late responses (125 and 195 ms) are reduced in magnitude (see Figure 4L). These differences are not resulting from differences in saccade duration as their mean values did not differ significantly (Figure 4J; rank-sum test: $z = -0.21$, $p = 0.83$). Instead, the differences reflect a drop in scalp voltage amplitude in the fog conditions as well as a delay of the saccade-related TRF activity seen around 195 ms (see Figure 4K). The drop in amplitude may also be due to increased jitter.

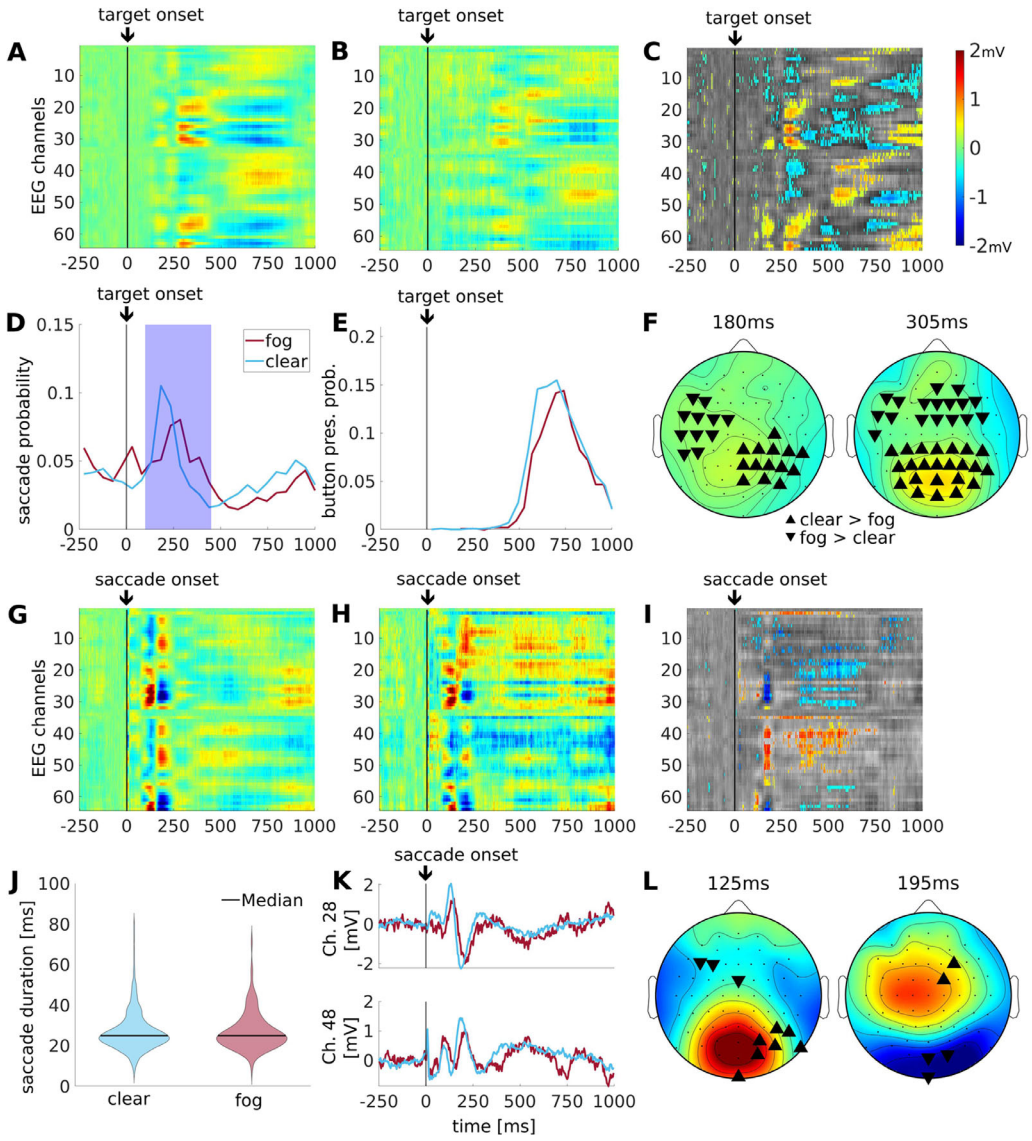

Figure 4. **Target visibility: difference between clear and poor stimulus visibility.** All trials here had button responses. (**A**) Target-locked TRF in the clear visibility condition ($N = 3159$) shows an earlier and higher amplitude response relative to that in the panel (**B**) the fog condition ($N = 876$). (**C**) Differences in target-locked TRFs in the two visibility conditions (clear and fog). Significant differences are shown in color, superimposed on non-significant differences in gray. (**D**) Saccade histograms for fog and clear visibility conditions. Subjects' saccade to target significantly later in the clear compared to the fog condition. Target-evoked saccades (blue shaded time interval, 100–450 ms) are selected for the saccade-locked comparison of the clear and fog visibility conditions (pertinent to panels **G–L**). (**E**) Similarly subjects' button press responses are also significantly later in the clear compared to the fog condition. (**F**) Topographic snapshots at 180 ms and 305 ms show the spatial distribution of the differences in panel **C**. (**G**) Saccades-locked TRF to clear condition ($N = 1382$) show a strong response but this is absent in the panel (**H**) fog condition ($N = 367$). (**I**) Comparing the condition in the saccade-locked TRFs shows a contrast strongly driven by the saccade responses for clear visibility. Significant differences are shown in color, superimposed on nonsignificant differences in gray. (**J**) Density plots of saccade duration times for the clear and fog condition saccades. (**K**) EEG traces for channels 28 and 48 showing the significance between clear (blue) and fog (red) is driven by higher amplitude and the earlier neural response of the clear condition. Color map indicates mV identically in all panels **A** to **C**, **F**, **G** to **I**, and **L**), however, in panels **C** and **I**, the color indicates voltage difference between visibility conditions. (**L**) At 125 ms and 195 ms this result is spatially similar to Figure 3F.

Peripheral targets elicit stronger saccade-locked TRFs, without affecting response times

We also expected that targets appearing in the periphery of vision would elicit larger saccades, and possibly differ in how the target is processed. To test for this, targets were split into equal numbers of "peripheral targets" and "central targets" depending on the distance between the subject's gaze and the location of the target when it first appeared on the screen. The median distance for this split was 8.58 degrees in visual angle (median established over all trials across all subjects). Subjects may have saccading earlier for central targets (see Figure 5A; 100–450 ms after target onset; signed-rank test: $z(15) = -1.45$, $p = 0.15$) and had a larger number of detected saccades (see Figure 5A, signed-rank test: $z(15) = -3.52$, $p = 4e{-}04$). Saccade durations showed no significant difference (see Figure 5G; rank-sum test: $z = -1.26$, $p = 0.207$). Additionally, there was no significant difference in mean button response times (see Figure 5E, signed-rank test: $z(15) = -1.34$, $p = 0.18$). However, they responded more frequently (see Figure 5D) and with higher accuracy to the central targets (see Figure 5I, signed-rank test: $z(15) = -3.10$, $p = 0.0019$). We find significant differences in target-related TRF

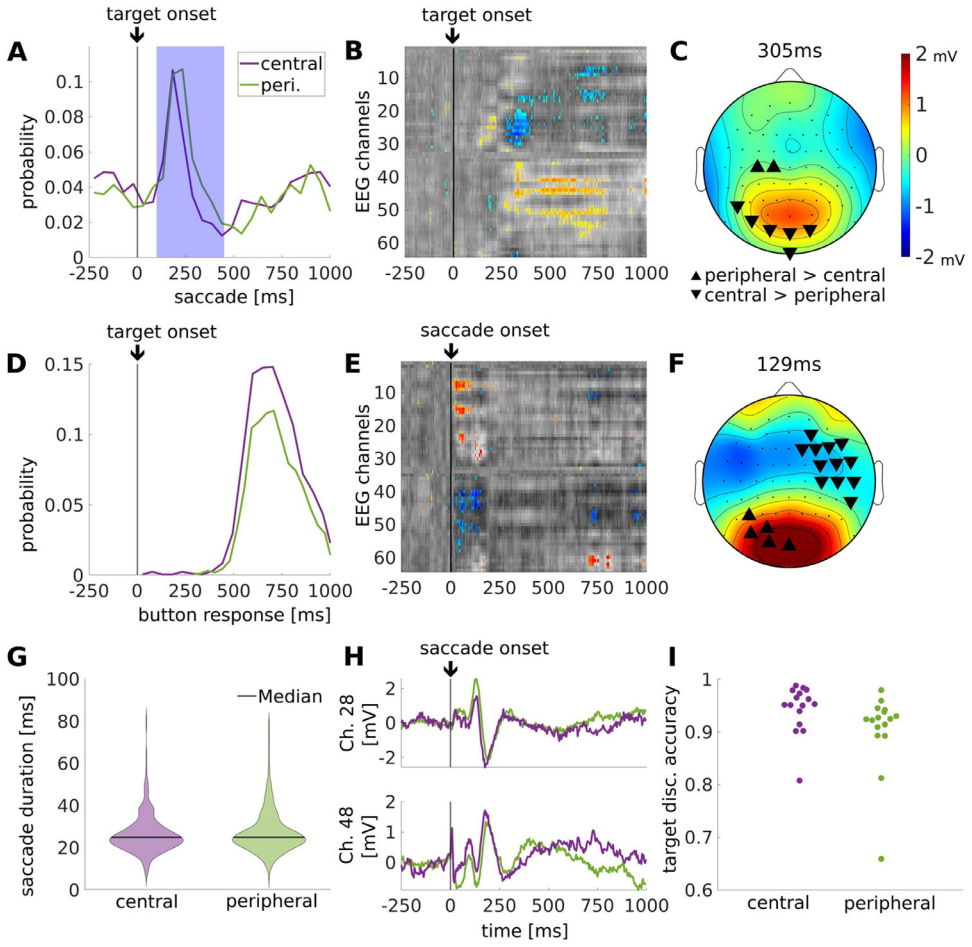

Figure 5. **Target location: differences between responses to peripheral and central targets.** (**A**) Saccade time histograms relative to target onset. Target-evoked saccades (blue shaded time interval, 100–450 ms) are selected for the saccade-locked comparison of the central and peripheral targets (pertinent to panels **E–I**). (**B**) Difference in target-locked TRF, taking peripheral ($N = 1546$) minus central ($N = 1613$) target locations. Significant differences are shown in color, superimposed on nonsignificant differences in gray. (**C**) Topographic snapshot of target-locked TRF at 305 ms. (**D**) Button response histogram locked to target onset for central and peripheral targets. (**E**): Difference in saccade-locked TRF between peripheral ($N = 830$) minus central ($N = 552$) targets. (**F**) Topographic snapshot of saccade-locked TRF at 129 ms. (**G**) Distribution of saccade duration for the central and peripheral targets (rank-sum test: $z = -1.26$, $p = 0.21$). (**H**) TRF for channels 28 and 48 showing that differences in panel **E** are due to differences in amplitude between peripheral (green) and central (violet) targets. (**I**) Button response accuracy for central or peripheral targets. The color map indicates mV identically in all panels **B**, **C**, **E**, and **F**, however, in panels **B** and **E**, the color indicates voltage difference between types target locations.

between the peripheral and central targets starting at 305 ms (see Figures 5B, 5C), which is shortly after the majority of saccades have terminated. We also did find differences in saccade-locked TRF at starting with saccade onset and including the activity we previously observed at 125 ms (see Figures 5E, 5F; here, differences are more apparent at 129 ms). In total, equal response time, as well as an effect of pre-saccade target location on evoked response suggests that processing of the target started prior to saccade onset.

In closing, we want to note that the results reported in Figures 3 to 5 were all computed in the "easy" game condition, and reported here only if they reproduced similarly for the "hard" game conditions (see Supplementary Figures S4, S5, S6), as no significant differences between easy and hard game conditions were found. We also did not find differences between threat and no-threat targets that were consistent across game difficulty (Supplementary Figure S7).

Discussion

To summarize, targets appearing suddenly in a dynamic visual scene elicit immediate saccades. An early evoked potential (at 125 ms) following the onset of these saccades is modulated by visibility as well as the location of the target. This suggests that visual processing of the target continues throughout the period of the ensuing saccade. A late evoked potential (195 ms) following the onset of these saccades is not present during spontaneous saccades and has a scalp distribution reminiscent of the classic P300.

Here, we made an attempt to separate neural activity evoked by the target from neural activity associated with saccades. This is complicated by the fact that the target presentation is reliably followed by saccades. Essentially, we extract activity locked to either target onset or saccade onset, while removing correlation induced by their overlapping co-occurrence. Interestingly, the presence and properties of a target modify the activity evoked by saccades, despite having removed target-locked activity. This finding implies that the presence of a target has a continued effect on stimulus processing after saccades. A caveat of this study is that we did not manipulate the stimulus during the saccades. Therefore, we cannot make any specific claims about saccadic suppression of visual input typically observed for stimuli presented during a saccade (Reingold & Stampe, 2002).

Differences in peak neural activity between target and spontaneous saccades are most evident 195 ms after saccade onset. The peak response at this time has a distribution similar to the well known P300, specifically the P3a (Polich, 2007). Similar to the conventional P3a, it peaks at approximately 400 ms after target onset. Remarkably, this activity does not appear with that same spatial distribution in the target evoked activity (i.e. locked to the target presentation). There is previous evidence that the P300 occurs after a saccade onto a target (Brouwer et al., 2013; Devillez et al., 2015) and does not fundamentally differ from that found under conventional fixation conditions (Dandekar, Ding, Privitera, Carney, & Klein, 2012). During free viewing, the timing of the P300 seems to depend on the difficulty of detecting a target among distractors (e.g. for targets crowded by distractors), discriminant activity appears 480 ms after fixation (Kamienkowski, Ison, Quiroga, & Sigman, 2012) but already at 180 ms for less crowded targets in natural images (Kamienkowski, Varatharajah, Sigman, & Ison, 2018; i.e. with a similar timing and spatial distribution to the activity observed here at 195 ms after saccade onset). However, the present experiment did not have distractors or standard events as subjects are instructed to respond to all targets, threat and no-threat alike. Therefore, we cannot confirm that this activity follows the expected behavior of a P3a, such as a dependence on target expectancy (Polich, 2007). The alternative interpretation of this activity is that it is associated with the target detection itself. Such target-detection potentials have been previously reported with a similar spatial distribution in the context of fixation-related potentials (Huber-Huber, Buonocore, Dimigen, Hickey, & Melcher, 2019; Buonocore, et al., 2020). We favor the interpretation of this activity at 195 ms post saccade as a marker of surprise. Remarkably, this activity does not appear with that same spatial distribution in the target evoked activity (i.e. locked to the target presentation). Therefore, regardless of the interpretation, we find an early response temporally coupled to the saccade (i.e. the reorienting event), rather than the target presentation itself.

We argue for the primacy of saccade-related processing, as opposed to target-related processing. Yet, we find a clear early effect of the target stimulus on the saccade related potentials, specifically, visibility, and screen location (i.e. clear and fog, and central and peripheral targets). Visibility in the clear and fog conditions in our study is most closely related to contrast variations in traditional studies. The activity found at 125 ms is consistent in timing and spatial distribution with early visual responses. Specifically, the C1 occipital negativity peaks 75 ms after stimulus presentation (Clark et al., 1994) and its magnitude increases with stimulus contrast (Foxe, Strugstad, Sehatpour, Molholm, Pasieka, Schroeder, & McCourt, 2008; Gebodh, Vanegas, & Kelly, 2017). Note that this component is measured relative to the onset of a peripheral stimulus during fixation. Given the approximate 30 ms average saccade duration in our study, the contrast dependence we see at 125 ms after saccade onset can readily be explained as

modulation of visual processing starting with fixation onset.

Interestingly, the spatial distribution of this post-saccadic activity is consistent with the traditional C1 response, which has occipital positivity for visual stimuli appearing in the lower visual field (Gebodh et al., 2017). This is consistent with targets appearing laterally below the mean fixation point. In contrast to the TRF associated with target-evoked saccades, the TRF associated with target appearance does not match conventional visual evoked responses, neither in timing nor spatial distribution. Thus, saccade TRFs are a better match to early visual processing under fixation conditions than conventional stimulus-evoked TRFs.

Although contrast dependence of the early activity may result from post-saccadic processing, the dependence on the location is harder to explain. After both peripheral and central saccades subjects are foveating the target, and therefore visual input after fixation onset is approximately the same. Therefore, the location dependence suggests that visual processing of the target starts prior to the saccade and has a delayed influence on visual processing at 129 ms after the saccade. The fact that button response times are independent of where the target appears on the screen also suggests that target processing is undisturbed by the intervening saccades.

A similar picture emerges if we interpret this activity as part of the lambda complex. The lambda complex is an evoked activity found in the fixation-locked analysis. It has a dominant positive deflection over occidental electrodes after fixation, appearing at 125 to 140 ms when the saccade locked (Yagi, 1979). For relatively short saccades of 30 ms, it is expected to be at 100 to 125 ms (Thickbroom, Knezevic, Carroll, & Mastaglia, 1991). Its neural generator is thought to be the same as early occipital responses in the conventional stimulus-evoked analysis (Kazai & Yagi, 2003). Because the lambda response is known to be sensitive to the afferent sensory input at fixation (Ries, Slayback, & Touryan, 2018; Yagi, 1981) it could be argued that the larger saccade-locked activity found here is due to the differences in sensory information at fixation (e.g. luminance contrast of the target may be higher than spontaneous fixation locations). However, there are saccade-locked components at earlier latencies relative to the dominant lambda complex over occipital electrodes (Thickbroom et al., 1991), and there is support for a fixation-locked component at approximately 50 ms that differentiates salience/contrast (Fischer, Graupner, Velichkovsky, & Pannasch, 2013). This suggests that visual processing at the saccade target likely starts prior to fixation onset and makes the current findings hard to reconcile with purely post-saccade processing.

Previous work using classical paradigms of visual perception provide behavioral evidence that some amount of visual processing is preserved throughout the saccade (Fracasso, Caramazza, & Melcher, 2010; Irwin, Carlson-Radvansky, & Andrews, 1995). Neural evidence for continuous processing across saccades comes from recordings in non-human primates during constrained visual search tasks (Bichot, Rao, & Schall, 2001; Sheinberg & Logothetis, 2001). Effects of pre-saccadic stimulus on post-saccadic scalp potentials have been demonstrated in a variety of studies. For instance, the presence or spatial frequency of simple stimuli before a saccade is reflected in an occipital positivity 50 to 75 ms after fixation onset (Bellebaum & Daum, 2006; Kazai & Yagi, 1999). These have been interpreted as signals related to the updating of retinal location (Peterburs et al., 2011) leveraging an efference copy, consistent with a saccade-lock of this early contrast.

More recent work emphasizes predictive processing based on the pre-saccadic stimulus. For instance, if a pre-saccade stimulus changes during a saccade, occipital electrodes show differences starting at 200 ms after the saccade (Ehinger et al., 2015). Similarly, during reading, upcoming words that appear in the periphery affect occipital electrodes when they are fixated after a saccade (Dimigen et al., 2012). A recent study on face perception shows that a scrambled face presented in the periphery prior to fixation decreases responses starting at 180 ms post-fixation (Buonocore et al., 2020; Huber-Huber et al., 2019). The picture that emerges from these studies is that the pre-saccadic stimulus primes visual processing after the subsequent saccade. These experiments were all conducted with highly constrained stimuli and tasks. Here, with an unconstrained detection task and relatively naturalistic dynamic stimulus, we find both an early effect of the pre-saccade target location, as well as a later response likely associated with surprise.

One caveat to our conclusions is that the lambda complex is modulated by saccade amplitude (Yagi, 1979). The method we used to detect saccades based on EOG had the advantage that it detected saccades of approximately the same duration, and, hence, size (Bahill, Clark, & Stark, 1975).

We generally found no differences in saccade duration in all the contrasts we performed. We did, however, find differences in saccade-locked TRFs starting with saccade onset, in the contrast between peripheral and central targets. This is likely the result of differences in saccade dynamics. However, given the lack of a difference in saccade duration, it is unlikely that amplitude differences after the saccade (at 129 ms) are the result of altered saccade dynamics. Another caveat to our study is that we were not able to detect and analyze smaller saccades, which may have differed between these two conditions.

Although much of the literature on the lambda complex is locked to fixation onset, here, we favored

the saccade onset because it is more clearly defined in time in the EOG, which we use to detect saccades and fixations. In general, saccade-related signals are more time accurate, as compared to fixation-related signals (e.g. Katz, Patel, Talakoub, Groppe, Hoffman, & Valiante, 2020). Nevertheless, given the close correspondence of the saccade and fixation locked lambda (Thickbroom et al., 1991), we expect, however, that most results would remain if we had performed a fixation-locked analysis. We recommend recording eye position with sufficient temporal and spatial resolution to detect saccades onset and offset, to overcome the limitation of the present study.

Conclusion

The literature suggests a continuity of visual perception during saccades, with processing starting prior, a saccadic suppression during, and an enhancement after the saccade. This existing work largely used discrete stimuli and constrained eye movements. Here, we used a target detection task embedded in a video game to provide a more naturalistic setting with free viewing. We find that the presence of the target, its visibility, and its location affect neural responses early after the saccade. Overall, we conclude that during natural viewing of dynamic scenes, neural processing of the visual stimuli, including orienting, starts before a saccade and continues throughout the saccade, apparently unencumbered by saccadic suppression. A major contribution of this work is the evidence for continuity of visual processing throughout the saccade during free viewing in a realistic environment in humans.

Methodologically, the results of the present study steer the conversation away from visual evoked responses locked to the timing of stimulus presentation and toward a focus on eye movements and their essential relation to task engagement, which motivates where we look. We hope that the system identification approach used here to disentangle overlapping neural activity will benefit future research into ecologically valid tasks and stimuli.

Keywords: free viewing, natural dynamic stimuli, saccade, electroencephalogram (EEG), temporal response function (TRF), active sensing

Acknowledgments

The authors thank Maximilian Nentwich for his technical and intellectual input concerning data analysis, data interpretation, and core scientific ideas.

Funding source: ARL/DSO W911NF-10-2-0022 (Subaward from DCS Corp: APX02-N013).

Commercial relationships: none.
Corresponding author: Atanas D. Stankov
Email: astankov@gradcenter.cuny.edu.
Address: Department of Biomedical Engineering, City College of New York, 160 Convent Avenue, New York, NY 10031, USA.

References

Bahill, A. T., Clark, M. R., & Stark, L. (1975). The main sequence, a tool for studying human eye movements. *Mathematical Biosciences, 24*(3), 191–204.

Barczak, A., Haegens, S., Ross, D. A., McGinnis, T., Lakatos, P., & Schroeder, C. E. (2019). Dynamic Modulation of Cortical Excitability during Visual Active Sensing. *Cell Reports, 27*(12), 3447–3459.e3.

Bellebaum, C., & Daum, I. (2006). Time course of cross-hemispheric spatial updating in the human parietal cortex. *Behavioural Brain Research, 169*(1), 150–161.

Benjamini, Y., & Hochberg, Y. (1995). Controlling the False Discovery Rate: A Practical and Powerful Approach to Multiple Testing. *Journal of the Royal Statistical Society: Series B (Methodological), 57*(1), 289–300.

Bichot, N. P., Rao, S. C., & Schall, J. D. (2001). Continuous processing in macaque frontal cortex during visual search. *Neuropsychologia, 39*(9), 972–982.

Brouwer, A.-M., Reuderink, B., Vincent, J., van Gerven, M. A. J., & van Erp, J. B. F. (2013). Distinguishing between target and nontarget fixations in a visual search task using fixation-related potentials. *Journal of Vision, 13*(3), 17.

Buonocore, A., Dimigen, O., & Melcher, D. (2020). Post-Saccadic Face Processing Is Modulated by Pre-Saccadic Preview: Evidence from Fixation-Related Potentials. *Journal of Neuroscience, 40*(11), 2305–2313.

Candès, E. J., Li, X., Ma, Y., & Wright, J. (2011). Robust principal component analysis? *Journal of the ACM, 58*(3), Article 11, Publication date: May 2011.

Castet, E., & Masson, G. S. (2000). Motion perception during saccadic eye movements. *Nature Neuroscience, 3*(2), 177–183.

Clark, V. P., Fan, S., & Hillyard, S. A. (1994). Identification of early visual evoked potential

generators by retinotopic and topographic analyses. *Human Brain Mapping, 2*(3), 170–187.

Crosse, M. J., Di Liberto, G. M., Bednar, A., & Lalor, E. C. (2016). The Multivariate Temporal Response Function (mTRF) Toolbox: A MATLAB Toolbox for Relating Neural Signals to Continuous Stimuli. *Frontiers in Human Neuroscience, 10*, 604.

Dandekar, S., Ding, J., Privitera, C., Carney, T., & Klein, S. A. (2012). The Fixation and Saccade P3. *PLoS One, 7*(11), e48761.

Dandekar, S., Privitera, C., Carney, T., & Klein, S. A. (2011). Neural saccadic response estimation during natural viewing. *Journal of Neurophysiology, 107*(6), 1776–1790.

Deubel, H. (2008). The time course of presaccadic attention shifts. *Psychological Research, 72*(6), 630.

Devillez, H., Guyader, N., & Guérin-Dugué, A. (2015). An eye fixation–related potentials analysis of the P300 potential for fixations onto a target object when exploring natural scenes. *Journal of Vision, 15*(13), 20.

Dias, J. C., Sajda, P., Dmochowski, J. P., & Parra, L. C. (2013). EEG precursors of detected and missed targets during free-viewing search. *Journal of Vision, 13*(13), 13.

Dimigen, O., & Ehinger, B. V. (2021). Regression-based analysis of combined EEG and eye-tracking data: Theory and applications. *Journal of Vision, 21*(1), 3.

Dimigen, O., Kliegl, R., & Sommer, W. (2012). Trans-saccadic parafoveal preview benefits in fluent reading: A study with fixation-related brain potentials. *NeuroImage, 62*(1), 381–393.

Dorr, M., & Bex, P. J. (2013). Peri-Saccadic Natural Vision. *Journal of Neuroscience, 33*(3), 1211–1217.

Dorr, M., Martinetz, T., Gegenfurtner, K. R., & Barth, E. (2010). Variability of eye movements when viewing dynamic natural scenes. *Journal of Vision, 10*(10), 28.

Ehinger, B. V., König, P., & Ossandón, J. P. (2015). Predictions of Visual Content across Eye Movements and Their Modulation by Inferred Information. *Journal of Neuroscience, 35*(19), 7403–7413.

Fischer, T., Graupner, S.-T., Velichkovsky, B. M., & Pannasch, S. (2013). Attentional dynamics during free picture viewing: Evidence from oculomotor behavior and electrocortical activity. *Frontiers in Systems Neuroscience, 7*, 17.

Foxe, J. J., Strugstad, E. C., Sehatpour, P., Molholm, S., Pasieka, W., Schroeder, C. E., … McCourt, M. E. (2008). Parvocellular and Magnocellular Contributions to the Initial Generators of the Visual Evoked Potential: High-Density Electrical Mapping of the "C1" Component. *Brain Topography, 21*(1), 11–21.

Fracasso, A., Caramazza, A., & Melcher, D. (2010). Continuous perception of motion and shape across saccadic eye movements. *Journal of Vision, 10*(13), 14.

Gebodh, N., Vanegas, M. I., & Kelly, S. P. (2017). Effects of Stimulus Size and Contrast on the Initial Primary Visual Cortical Response in Humans. *Brain Topography, 30*(4), 450–460.

Gordon, S. M., Jaswa, M., Solon, A. J., & Lawhern, V. J. (2017). Real World BCI: Cross-Domain Learning and Practical Applications. *Proceedings of the 2017 ACM Workshop on An Application-Oriented Approach to BCI out of the Laboratory - BCIforReal '17*, 25–28. Limassol, Cyprus.

Guérin-Dugué, A., Roy, R. N., Kristensen, E., Rivet, B., Vercueil, L., & Tcherkassof, A. (2018). Temporal Dynamics of Natural Static Emotional Facial Expressions Decoding: A Study Using Event- and Eye Fixation-Related Potentials. *Frontiers in Psychology, 9*, 1190.

Hiebel, H., Ischebeck, A., Brunner, C., Nikolaev, A. R., Höfler, M., & Körner, C. (2018). Target probability modulates fixation-related potentials in visual search. *Biological Psychology, 138*, 199–210.

Huber-Huber, C., Buonocore, A., Dimigen, O., Hickey, C., & Melcher, D. (2019). The peripheral preview effect with faces: Combined EEG and eye-tracking suggests multiple stages of trans-saccadic predictive and non-predictive processing. *NeuroImage, 200*, 344–362.

Ibbotson, M., & Krekelberg, B. (2011). Visual perception and saccadic eye movements. *Current Opinion in Neurobiology, 21*(4), 553–558.

Ibbotson, M. R., Crowder, N. A., Cloherty, S. L., Price, N. S. C., & Mustari, M. J. (2008). Saccadic Modulation of Neural Responses: Possible Roles in Saccadic Suppression, Enhancement, and Time Compression. *Journal of Neuroscience, 28*(43), 10952–10960.

Irwin, D. E., Carlson-Radvansky, L. A., & Andrews, R. V. (1995). Information processing during saccadic eye movements. *Acta Psychologica, 90*(1), 261–273.

Jonikaitis, D., Szinte, M., Rolfs, M., & Cavanagh, P. (2012). Allocation of attention across saccades. *Journal of Neurophysiology, 109*(5), 1425–1434.

Kamienkowski, J. E., Ison, M. J., Quiroga, R. Q., & Sigman, M. (2012). Fixation-related potentials in visual search: A combined EEG and eye tracking study. *Journal of Vision, 12*(7), 4.

Kamienkowski, J. E., Varatharajah, A., Sigman, M., & Ison, M. J. (2018). Parsing a mental program: Fixation-related brain signatures of unitary

operations and routines in natural visual search. *NeuroImage, 183*, 73–86.

Katz, C. N., Patel, K., Talakoub, O., Groppe, D., Hoffman, K., & Valiante, T. A. (2020). Differential Generation of Saccade, Fixation, and Image-Onset Event-Related Potentials in the Human Mesial Temporal Lobe. *Cerebral Cortex, 30*(10), 5502–5516.

Kazai, K., & Yagi, A. (1999). Integrated effect of stimulation at fixation points on EFRP (eye-fixation related brain potentials). *International Journal of Psychophysiology, 32*(3), 193–203.

Kazai, K., & Yagi, A. (2003). Comparison between the lambda response of eye-fixation-related potentials and the P100 component of pattern-reversal visual evoked potentials. *Cognitive, Affective, & Behavioral Neuroscience, 3*(1), 46–56.

Konstantopoulos, P., Chapman, P., & Crundall, D. (2010). Driver's visual attention as a function of driving experience and visibility. Using a driving simulator to explore drivers' eye movements in day, night and rain driving. *Accident Analysis & Prevention, 42*(3), 827–834.

Lalor, E. C., Pearlmutter, B. A., Reilly, R. B., McDarby, G., & Foxe, J. J. (2006). The VESPA: A method for the rapid estimation of a visual evoked potential. *NeuroImage, 32*(4), 1549–1561.

MacEvoy, S. P., Hanks, T. D., & Paradiso, M. A. (2008). Macaque V1 Activity During Natural Vision: Effects of Natural Scenes and Saccades. *Journal of Neurophysiology, 99*(2), 460–472.

Marton, M., Szirtes, J., & Breuer, P. (1985). Late components of lambda responses in cognitive tasks. *Documenta Ophthalmologica, 59*(2), 199–204.

Novitskiy, N., Ramautar, J. R., Vanderperren, K., De Vos, M., Mennes, M., Mijovic, B., Vanrumste, B., Stiers, P., Van den Bergh, B., Lagae, L., Sunaert, S., Van Huffel, S., . . . Wagemans, J. (2011). The BOLD correlates of the visual P1 and N1 in single-trial analysis of simultaneous EEG-fMRI recordings during a spatial detection task. *NeuroImage, 54*(2), 824–835.

Otero-Millan, J., Troncoso, X. G., Macknik, S. L., Serrano-Pedraza, I., & Martinez-Conde, S. (2008). Saccades and microsaccades during visual fixation, exploration, and search: Foundations for a common saccadic generator. *Journal of Vision, 8*(14), 21.

Peterburs, J., Gajda, K., Hoffmann, K.-P., Daum, I., & Bellebaum, C. (2011). Electrophysiological correlates of inter- and intrahemispheric saccade-related updating of visual space. *Behavioural Brain Research, 216*(2), 496–504.

Polich, J. (2007). Updating P300: An integrative theory of P3a and P3b. *Clinical Neurophysiology, 118*(10), 2128–2148.

Purcell, B. A., Heitz, R. P., Cohen, J. Y., & Schall, J. D. (2012). Response variability of frontal eye field neurons modulates with sensory input and saccade preparation but not visual search salience. *Journal of Neurophysiology, 108*(10), 2737–2750.

Rämä, P., & Baccino, T. (2010). Eye fixation–related potentials (EFRPs) during object identification. *Visual Neuroscience, 27*(5–6), 187–192.

Reingold, E. M., & Stampe, D. M. (2002). Saccadic Inhibition in Voluntary and Reflexive Saccades. *Journal of Cognitive Neuroscience, 14*(3), 371–388.

Ries, A. J., Slayback, D., & Touryan, J. (2018). The fixation-related lambda response: Effects of saccade magnitude, spatial frequency, and ocular artifact removal. *International Journal of Psychophysiology, 134*, 1–8.

Ross, J., Morrone, M. C., & Burr, D. C. (1997). Compression of visual space before saccades. *Nature, 386*(6625), 598–601.

Ross, J., Morrone, M. C., Goldberg, M. E., & Burr, D. C. (2001). Changes in visual perception at the time of saccades. *Trends in Neurosciences, 24*(2), 113–121.

Sheinberg, D. L., & Logothetis, N. K. (2001). Noticing Familiar Objects in Real World Scenes: The Role of Temporal Cortical Neurons in Natural Vision. *Journal of Neuroscience, 21*(4), 1340–1350.

Thickbroom, G. W., Knezevic̆, W., Carroll, W. M., & Mastaglia, F. L. (1991). Saccade onset and offset lambda waves: Relation to pattern movement visually evoked potentials. *Brain Research, 551*(1), 150–156.

Toivanen, M., Pettersson, K., & Lukander, K. (2015). A probabilistic real-time algorithm for detecting blinks, saccades, and fixations from EOG data. *Journal of Eye Movement Research, 8*(1), 1–14.

Yagi, A. (1979). Saccade size and lambda complex in man. *Physiological Psychology, 7*(4), 370–376.

Yagi, A. (1981). Visual signal detection and lambda responses. *Electroencephalography and Clinical Neurophysiology, 52*(6), 604–610.